



Cognitive Design of Radar Waveform and the Receive Filter for Multitarget Parameter Estimation

Yu Yao¹ · Junhui Zhao¹ · Lenan Wu²

Received: 1 June 2018 / Accepted: 18 December 2018 / Published online: 8 January 2019
© Springer Science+Business Media, LLC, part of Springer Nature 2019

Abstract

This research work considers waveform design for an adaptive radar system. The aim is to achieve enhanced feature extraction performance for multiple extended targets. There are two scenarios to consider: multiple extended targets separated in range and multiple extended targets close in range. We propose a waveform optimization scheme based on Kalman filtering by minimizing the mean square error of separated target scattering coefficient estimation and a waveform optimization approach by minimizing the mean square error of closed power spectrum density estimation. A convex cost function is established, and the optimal solution can be obtained using the existing convex programming algorithm. With subsequent iterations of the algorithm, the simulation results demonstrate an improvement in the estimation of target parameters from the dynamic scene, such as target scattering coefficient and power spectrum density, while maintaining relatively lower computational complexity.

Keywords Kalman filtering · Target scattering coefficient estimation · Power spectrum density estimation · Waveform optimization · Multiple extended targets

Mathematics Subject Classification 15A69 · 81P40 · 90C3

Communicated by Jyh-Horng Chou.

✉ Yu Yao
shell8696@hotmail.com
Junhui Zhao
junhuizhao@hotmail.com
Lenan Wu
wuln@seu.edu.cn

¹ East China Jiaotong University, Nanchang, China

² Southeast University, Nanjing, China

1 Introduction

Cognitive radar (CR) has received much attention in recent years. Similar to brain-empowered system architectures, CR employs the adaptive feedback principle to facilitate adaptive detection of the time-varying target scene [1–3]. Subsequently, the target feature information in the backscatter signal is exploited to allocate the power or spectrum of the probing signal at the transmitter [4, 5]. CR usually forms a closed feedback from the receiver to the transmitter. It is able to adaptively adjust probing signals or the receiver to suit the time-variant target scene [6, 7]. The feedback loop has great potential for improving the performance of target recognition and detection, as demonstrated in [8, 9]. Augusto and Antonio developed joint design of the transmit waveform and receive filter in the presence of noise interference [10]. Seyyed and Augusto consider that multiple-input-multiple-output (MIMO) radar utilizes information provided by a dynamic environmental database. The authors discussed designs of the space–time transmit code and space–time receive filter in the presence of noise interference [11]. Reference [12] proposed a novel method to design transmit waveforms sharing desirable spectral features, which ensure coexistence with wireless networks and optimal performance of target detection.

The transmitted waveforms of the CR are constantly adjusted in order to extract target feature information in a time-variant environment [13]. Many methods in several recent works have been proposed to design the cognitive waveform. The literature [14] developed waveform design methods, which provide good performance in terms of target resolution. Reference [15] proposed the design of the transmit waveform with aperiodic autocorrelation properties in terms of peak sidelobe level and integrated sidelobe level. Bell [16] discussed the waveform design problem for extended target detection and parameter estimation. Considering that the received signals are interfered with by the clutter noise, several waveform design algorithms are proposed by maximizing the signal-to-interference plus noise ratio (SINR) of the output signal [17, 18]. The CR waveform is optimized by maximizing the probability of target detection instead of the SINR of the output signal [19]. The corresponding algorithm is also discussed in the literature [20–22]. Under the condition of a given transmitted power constraint, the water-filling method is presented to allocate the transmitted power and maximize the mutual information [23–25]. Cognitive waveform design has been studied for improving the performance of target estimation and identification [26, 27]. The information theoretic criterion is generally used for target estimation [28]. For instance, references [29, 30] propose to minimize the mutual information (MI) between the echo waveform and the estimate of target impulse response (TIR). References [31, 32] propose minimization of the MSE of the TIR estimation.

Reference [33], which exploits temporal correlation of target response to obtain a good performance of target parameter estimation, proposed a scheme based on the Kalman filtering method. However, low reliability and high complexity were caused by the convolution operation in the time domain. The estimation of target scattering coefficients (TSCs) has received significant attention in recent studies of radar systems. References [34–36] are focused on maximizing the signal-to-noise ratio (SNR) of the backscattering signal or the MI between the backscattering signal and the TSC. However, TSC will continuously vary as the target and radar environment changes [37].

From the perspective of the cognitive system, the estimate of TSC should be updated to design CR waveforms constantly. Reference [38] presents a genetic algorithm based on the water-filling method to optimize the power spectrum density (PSD) of the transmit waveform for a single extended target. However, the computational complexity is high, and the algorithm is not practical. Optimization of the transmission waveform and the receiver impulse response is investigated by maximizing the probability of correct identification between two target classes [39].

Pursuant to the above discussion, we intend to improve the target feature extraction performance by minimizing the MSE of TSC estimation for separated targets, in addition to minimizing the MSE of target PSD estimation for closed targets. The first proposed waveform design algorithm is intended to improve the performance of the TSC estimation and is summarized as follows: (1) we extract the target feature information derived from successive received signals at the receiver. TSC can be considered as a temporally correlated function during the pulse repetition interval (PRI). (2) By utilizing this temporal correlation of TSC changes, the waveform design problem is modeled by minimizing the MSE of the TSC estimation. The MSE of the TSC estimation can be obtained during the Kalman filtering-based iteration process.

Compared with the TSC, the target PSD is robust to the size of the target range cell and target-radar orientation. When multiple extended targets are close to each other and the radar echoes from different targets are superimposed, a target PSD is employed to describe the target feature. The second waveform design algorithm is proposed to improve the performance of target PSD estimation. The optimization process is preceded by target PSD estimation. The target PSD estimation is performed by the receiver. The receiver continually updates the target PSD estimation and uses the information to select the optimal waveform for illumination. An adaptive feedback loop enables the delivery of the estimated value of PSD to the transmitter. The transmitter adapts its transmitted waveform to suit the time-variant environment.

The main contributions of the research work are summarized as follows:

1. We present an adaptive radar system model based on the idea of the MSE of TSC or target PSD minimization.
2. We present a Kalman filtering-based waveform design approach by making use of the temporal correlation of TSC derived from successive received signals.
3. We provide performance analysis of the adaptive system in terms of TSC estimation and target PSD estimation by the proposed iteration steps. The proposed algorithm has relatively lower computational complexity.

The organization of this paper is as follows. In Sect. 2, a radar system model for multitarget parameter estimation is formulated. In Sect. 3, TSC estimation based on the maximum a posteriori (MAP) criterion is discussed. In Sect. 4, we propose a waveform optimization scheme based on Kalman filtering for separated targets by minimizing the MSE of TSC estimation and a waveform design scheme for closed targets by minimizing the MSE of target PSD estimation. The simulation results illustrating the proposed methods are provided in Sect. 5, and the conclusions are summarized in Sect. 6.

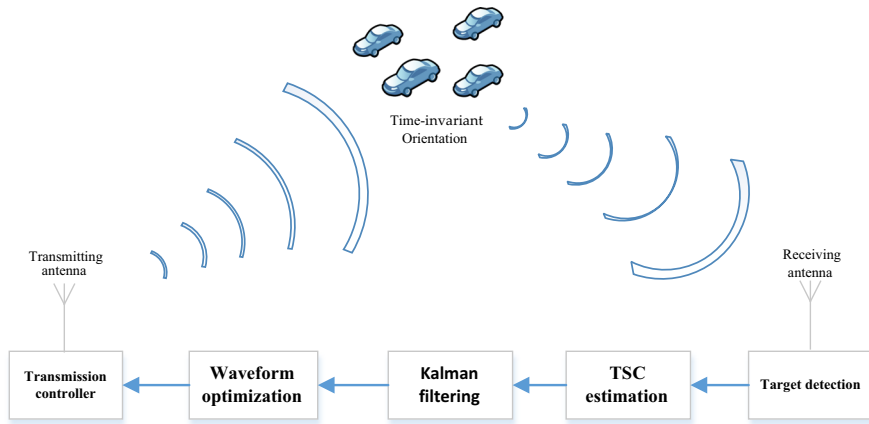


Fig. 1 Adaptive radar architecture for multiple target estimation

2 Radar System Model

In the intelligent transportation scenario, we analyze the performance of an adaptive radar system that contains the idea of “Kalman filtering” and “target estimation.” The system architecture of the adaptive radar is presented in Fig. 1. The system consists of four modules: the transceiver device, TSC estimation module, Kalman filtering module, and waveform optimization module. The Kalman filtering module and TSC estimation module are the novel schemes that distinguish the proposed adaptive system from a traditional feedback system.

Throughout this paper, vectors are denoted by boldface lowercase letters and matrices by boldface uppercase letters. In this work, a range-extended target can be modeled as a linear time-invariant system with a random impulse response. The TIR can be denoted by $q(m), m = 0, \dots, M - 1$, where M is the number of range cells. The movement of the target causes the angles to change between the targets and the radar, which causes fluctuations of the amplitudes and angles of the target echoes. Since these fluctuations are temporally correlated during the PRI, the extended targets can be described by a wide-sense stationary (WSS)-uncorrelated scattering model. The TIRs of different times in a short interval are correlated, and the correlation coefficient decreases with increasing time interval [33]. During the i th pulse, the time dynamic characteristic of the k th TIR can be described as

$$\mathbf{q}_{k,i} = e^{-T/\tau} \mathbf{q}_{k,i-1} + \mathbf{u}, \tag{1}$$

where i is the index of the radar pulses and k is the index of the extended target. The vector $\mathbf{q}_{k,i} = [q_{k,i}(1), q_{k,i}(2), \dots, q_{k,i}(M)]^T$ describes the k th TIR at time i . where $(\cdot)^T$ denotes the transpose. T denotes the radar pulse interval. τ denotes the temporal correlation of target impulse during PRI, which is determined by the change rate of the target angle. \mathbf{u} is zero-mean complex Gaussian noise. To simplify the discussion, we assume that the correlation coefficients of all K targets are τ .

During the i th pulse, the change in characteristic of the frequency spectrum can be expressed by TSC as follows:

$$\mathbf{g}_{k,i} = e^{-T/\tau} \mathbf{g}_{k,i-1} + \mathbf{v}, \quad (2)$$

where $\mathbf{g}_{k,i} = \mathbf{\Gamma} \mathbf{q}_{k,i}$ and $\mathbf{\Gamma}$ is the matrix of the Fourier transform. Similarly, \mathbf{v} is zero-mean complex Gaussian noise. We denote the waveform that will be emitted as $\mathbf{f}_i = [f_i(1), f_i(2), \dots, f_i(M)]^T$, where M is the number of samples. The target echo in the time domain is the convolution of the TIR with the transmit waveform, which is characterized by high computational cost. The complexity of waveform design is increased and cannot be solved efficiently. In this work, through Fourier transforms, the expressions in physical space are transformed into wave number space, which facilitates the application of many mathematical natures and principles. The backscattering signals in the frequency domain scattered by the k th target at time i disturbed by the AWGN \mathbf{w} can be expressed as follows:

$$\mathbf{y}_{k,i} = \mathbf{Z}_i \mathbf{g}_{k,i} + \mathbf{w}, \quad (3)$$

where $\mathbf{z}_i = \mathbf{\Gamma} \mathbf{f}_i$, and $\mathbf{Z}_i = \text{diag}\{\mathbf{z}_i\} \in \mathbb{C}^{M \times M}$, $\text{diag}(\cdot)$ denotes the diagonal matrix. Note that the model in Eq. (3) approximates the linear convolution with the circular convolution. We consider that the targets are dispersed from each other (maintain a distance between each other). We assume that $\mathbf{Y}_i = [\mathbf{y}_{1,i} \ \mathbf{y}_{2,i} \ \dots \ \mathbf{y}_{K,i}]$ and $\mathbf{G}_i = [\mathbf{g}_{1,i} \ \mathbf{g}_{2,i} \ \dots \ \mathbf{g}_{K,i}]$ are the matrices of the received signals and TSC, respectively; $\mathbf{W} = [\mathbf{w}_1 \ \mathbf{w}_2 \ \dots \ \mathbf{w}_K]$ is the AWGN matrix. As a result, the backscattering signals reflected from all K targets can be denoted as follows:

$$\mathbf{Y}_i = \mathbf{Z}_i \mathbf{G}_i + \mathbf{W}. \quad (4)$$

We consider that \mathbf{G}_i and \mathbf{W} are independent of each other. Since the range delay and the target locations are not useful for CR waveform design, they are ignored in this paper.

3 TSC Estimation Based on the MAP Criterion

From Ref. [35], the TSC estimation ability should also be considered to provide prior knowledge for the optimization of the next waveform in CR waveform design for target detection. We intend to estimate TSC for improving the performance of multitarget detection in the CR system. During the i th pulse sample, TSC estimation based on the MAP criterion can be written as follows:

$$\hat{\mathbf{G}}_i = \arg \max_{\mathbf{G}_i} p(\mathbf{G}_i | \mathbf{Y}_i) = \arg \max_{\mathbf{G}_i} \frac{p(\mathbf{Y}_i | \mathbf{G}_i) p(\mathbf{G}_i)}{p(\mathbf{Y}_i)}, \quad (5)$$

where

$$\begin{aligned}
 p(\mathbf{Y}_i|\mathbf{G}_i) &= \frac{1}{(2\pi)^{M/2}|\mathbf{C}_N|^{K/2}} \exp\left(-\frac{1}{2}(\mathbf{Y}_i - \mathbf{Z}_i\mathbf{G}_i)^H \mathbf{C}_N^{-1}(\mathbf{Y}_i - \mathbf{Z}_i\mathbf{G}_i)\right), \\
 p(\mathbf{G}_i) &= \frac{1}{(2\pi)^{M/2}|\mathbf{C}_T|^{K/2}} \exp\left(-\frac{1}{2}(\mathbf{G}_i)^H \mathbf{C}_T^{-1}\mathbf{G}_i\right),
 \end{aligned}
 \tag{6}$$

where $\mathbf{C}_N = E\{\mathbf{W}^H\mathbf{W}\}$ is the covariance matrix of the AWGN. $\mathbf{g}_i \sim \mathbf{N}(0, \mathbf{C}_T)$ describes a zero-mean complex Gaussian vector with covariance matrix \mathbf{C}_T (\mathbf{C}_T denotes the covariance matrix of \mathbf{g}_i). Substituting (6) into (5), TSC estimation based on the MAP criterion can be written as follows:

$$\hat{\mathbf{G}}_i = \mathbf{Q}_i \mathbf{Y}_i.
 \tag{7}$$

where

$$\mathbf{Q}_i = \left[(\mathbf{Z}_i)^H \mathbf{C}_N^{-1} \mathbf{Z}_i + \mathbf{C}_T^{-1} \right]^{-1} (\mathbf{Z}_i)^H \mathbf{C}_N^{-1}.
 \tag{8}$$

The MSE of TSC estimation based on the MAP criterion can be expressed as follows:

$$\begin{aligned}
 E \left\{ \left\| \hat{\mathbf{G}}_i - \mathbf{G}_i \right\|_2^2 \right\} &= \mathbf{Q}_i \left(\mathbf{Z}_i \mathbf{C}_T (\mathbf{Z}_i)^H + \mathbf{C}_T \right) (\mathbf{Q}_i)^H \\
 &\quad - \mathbf{Q}_i \mathbf{Z}_i \mathbf{C}_T - \mathbf{C}_T (\mathbf{Z}_i)^H (\mathbf{Q}_i)^H + \mathbf{C}_T,
 \end{aligned}
 \tag{9}$$

where $E\{\cdot\}$ denotes the expectation operator and $\|\cdot\|_2$ is the l_2 norm. The weighted sum of the normalized MSE at time i can be described as follows:

$$e_i = \frac{E \left\{ \left\| \hat{\mathbf{G}}_i \boldsymbol{\eta} - \mathbf{G}_i \boldsymbol{\eta} \right\|_2^2 \right\}}{E \left\{ \left\| \mathbf{G}_i \boldsymbol{\eta} \right\|_2^2 \right\}}.
 \tag{10}$$

The vector $\boldsymbol{\eta} = [\eta_1, \dots, \eta_K]^T$, ($\|\boldsymbol{\eta}\|_2^2 = 1$) is employed for distributing the target weights.

4 Waveform Optimization

4.1 Separated Targets

Considering the problem of separated targets estimation, we propose a scheme of the waveform optimization on the premise of ensuring TSC estimation precision, which can be summarized as follows:

In the first step, we extract an estimate of TSC derived from successive received signals in the previous time instant. A method based on the MAP criterion is adopted

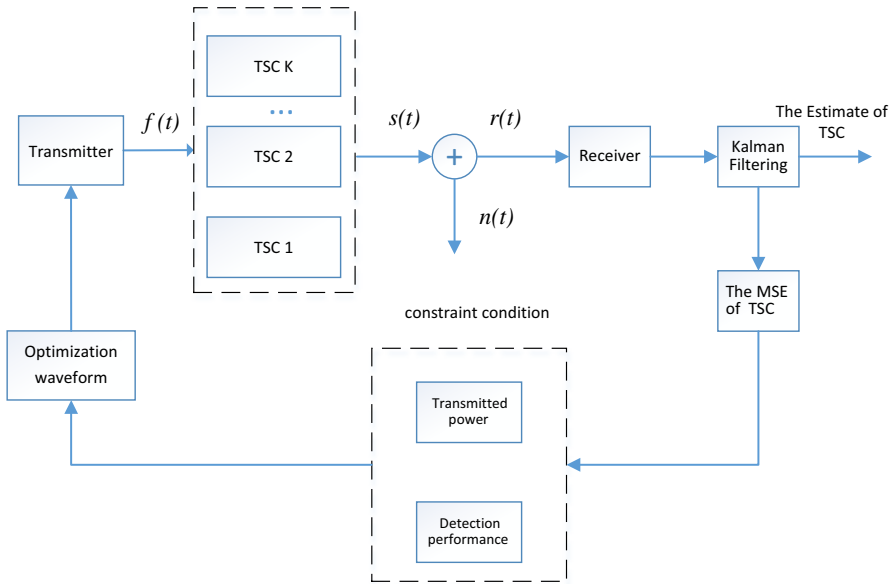


Fig. 2 The process of waveform optimization for TSC estimation

to estimate the current TSC. The MSE of TSC estimation can be obtained during the Kalman filtering-based iteration process.

In the second step, an optimization problem is modeled to design the transmit waveform by minimizing the MSE of the estimates of TSC, where a weight vector is introduced to achieve a trade-off among different targets.

The cognitive processing is summarized as follows. The receiver employs the Kalman filtering approach for updating the target parameters. The radar system updates the TSC estimation and utilizes this information to choose the optimal waveform for transmission. An adaptive feedback loop enables delivery of the estimate of TSC to the transmitter. The transmitter adapts its probing signals to suit the time-varying environment. The process of waveform optimization for TSC estimation is depicted in Fig. 2.

The TSC state transition and the observation process are denoted by Eqs. (2) and (4), respectively. The procedure of Kalman filtering for TSC estimation is summarized as Algorithm 1 in Table 1.

In parameter estimation, MSE is generally taken as the performance measurement. We develop a waveform optimization algorithm by minimizing the MSE of TSC estimation. During the i th pulse sample, the MSE of TSC estimation is preliminarily described as follows:

$$f(Z_i) = Tr\{\mathbf{P}_{i|i}\}, \tag{11}$$

Table 1 Kalman filtering for TSC estimation (Algorithm 1)

Initializing iteration index $i = 1$, the observed state of TSC $\hat{\mathbf{G}}_1 = \mathbf{Q}_1 \mathbf{Y}_1$ and the MSE of TSC $\mathbf{P}_{1|1} = 0$.

Step 1: The predicted matrix of TSC can be expressed as $\hat{\mathbf{G}}_{i|i-1} = e^{-T/\tau} \hat{\mathbf{G}}_{i-1|i-1}$.

Step 2: The predicted MSE of TSC can be obtained as $\mathbf{P}_{i|i-1} = e^{-2T/\tau} \mathbf{P}_{i-1|i-1} + (1 - e^{-2T/\tau}) \mathbf{C}_T$.

Step 3: The Kalman gain matrix can be expressed as $\Phi_i = \mathbf{P}_{i|i-1} (\mathbf{Q}_i \mathbf{Y}_i)^H \left[(\mathbf{Q}_i \mathbf{Y}_i) \mathbf{P}_{i|i-1} (\mathbf{Q}_i \mathbf{Y}_i)^H + \mathbf{Q}_i \mathbf{C}_N (\mathbf{Q}_i)^H \right]^{-1}$.

Step 4: The estimate of TSC can be expressed as $\hat{\mathbf{G}}_{i|i} = \hat{\mathbf{G}}_{i|i-1} + \Phi_i \mathbf{Q}_i \mathbf{Y}_i$.

Step 5: The MSE of TSC is updated as $\mathbf{P}_{i|i} = \mathbf{P}_{i|i-1} - \Phi_i \mathbf{Q}_i \mathbf{Y}_i \mathbf{P}_{i|i-1}$.

If $i = I_{\max}$, it ends; otherwise, we must repeat Step 1.

where $Tr\{\cdot\}$ denotes the trace of a matrix. Subject to transmitted power and detection probability constraints, the waveform design problem can be described as

$$\begin{aligned} & \min_{\mathbf{Z}_i} f(\mathbf{Z}_i) \\ & \text{s.t. } \|\mathbf{Z}_i\|_2^2 \leq E_f, \quad P_d \geq \varepsilon, \end{aligned} \tag{12}$$

where E_f describes the power of the transmitted waveform and P_d represents the probability of detection. The expression $P_d \geq \varepsilon$ can be expressed by $\mathbf{Z}_i^H \hat{\mathbf{G}}_i^H \mathbf{C}_N^{-1} \hat{\mathbf{G}}_i \mathbf{Z}_i \geq \varepsilon'$ (see [Appendix A](#)). From the literature [40], we can utilize the Woodbury identity to simplify the objective function. The objective function in (12) under the AWGN channel can be expressed by the trace of the MSE of estimates of TSC as follows:

$$\begin{aligned} f(\mathbf{Z}_i) &= Tr\{\mathbf{P}_{i|i}\} \\ &= Tr\left\{ \mathbf{P}_{i|i-1} - \mathbf{P}_{i|i-1} \mathbf{Z}_i^H \mathbf{Q}_i^H \left(\mathbf{Q}_i \mathbf{C}_T \mathbf{Q}_i^H + \mathbf{Q}_i \mathbf{Z}_i \mathbf{P}_{i|i-1} \mathbf{Z}_i^H \mathbf{Q}_i^H \right)^{-1} \mathbf{Q}_i \mathbf{Z}_i \mathbf{P}_{i|i-1} \right\} \\ &= Tr\left((\mathbf{P}_{i|i-1})^{-1} + \mathbf{Z}_i^H \mathbf{Q}_i^H \left(\mathbf{Q}_i \mathbf{C}_T \mathbf{Q}_i^H \right)^{-1} \mathbf{Q}_i \mathbf{Z}_i \right)^{-1} \\ &= Tr\left[(\mathbf{P}_{i|i-1})^{-1} + \mathbf{C}_T^{-1} - (\mathbf{C}_T + \mathbf{C}_T (\mathbf{Z}_i)^H \mathbf{C}_N^{-1} \mathbf{Z}_i \mathbf{C}_T)^{-1} \right]^{-1} \\ &\simeq Tr\left[\left((\mathbf{P}_{i|i-1})^{-1} + (\mathbf{Z}_i)^H \mathbf{C}_N^{-1} \mathbf{Z}_i \right)^{-1} \right]. \end{aligned} \tag{13}$$

The waveform optimization problem (12) can be rewritten as

$$\begin{aligned} \mathbf{Z}_i &= \min_{\mathbf{Z}_i} \left\{ Tr\left[\left((\mathbf{P}_{i|i-1})^{-1} + (\mathbf{Z}_i)^H \mathbf{C}_N^{-1} \mathbf{Z}_i \right)^{-1} \right] \right\} \\ & \text{s.t. } \|\mathbf{Z}_i\|_2^2 \leq E_f, \quad \mathbf{Z}_i^H \hat{\mathbf{G}}_i^H \mathbf{C}_N^{-1} \hat{\mathbf{G}}_i \mathbf{Z}_i \geq \varepsilon'. \end{aligned} \tag{14}$$

The objective function in (14) can be rewritten as

$$\begin{aligned}
 f(\mathbf{z}_i) &= Tr \left[\left((\mathbf{P}_{i|i-1})^{-1} + \text{diag}(\mathbf{z}_i)^H \mathbf{C}_N^{-1} \text{diag}(\mathbf{z}_i) \right)^{-1} \right] \\
 &= Tr \left[\left((\mathbf{P}_{i|i-1})^{-1} + \mathbf{U}_i \circ \mathbf{C}_N^{-1} \right)^{-1} \right], \tag{15}
 \end{aligned}$$

The symbol \circ is the Hadamard product. $\mathbf{U}_i = \mathbf{z}_i \mathbf{z}_i^H$, and $\mathbf{C}_N^{-1} = \begin{pmatrix} C_{1,1}^{-1} & \cdots & C_{1,K}^{-1} \\ \cdots & \cdots & \cdots \\ C_{M,1}^{-1} & \cdots & C_{M,K}^{-1} \end{pmatrix}$. Therefore, the above waveform design problem (12) is rewritten as

$$\begin{aligned}
 \mathbf{Z}_i &= \arg \min_{\mathbf{Z}_i} Tr \left[\left((\mathbf{P}_{i|i-1})^{-1} + \mathbf{U}_i \circ \mathbf{C}_N^{-1} \right)^{-1} \right] \\
 \text{s.t. } \mathbf{z}_i^H \mathbf{z}_i &\leq E_f, \quad p(\mathbf{z}_i) = \mathbf{z}_i^H \hat{\mathbf{G}}_i^H \mathbf{C}_N^{-1} \hat{\mathbf{G}}_i \mathbf{z}_i \geq \varepsilon', \tag{16}
 \end{aligned}$$

where \mathbf{U} is real and symmetric. The target detection constraint is described by $p(\mathbf{z}_i)$, which can achieve a maximum value via eigen-decomposition. \mathbf{z}_i is the eigenvector corresponding to the maximum eigenvalue of $\hat{\mathbf{G}}_i^H \mathbf{C}_N^{-1} \hat{\mathbf{G}}_i$; we have $p(\mathbf{z}_i) = \lambda_{\max} \mathbf{u}_{\max}^H \mathbf{u}_{\max}$, where λ_{\max} is the maximum eigenvalue of $\hat{\mathbf{G}}_i^H \mathbf{C}_N^{-1} \hat{\mathbf{G}}_i$ and \mathbf{u}_{\max} is the corresponding maximum eigenvector. $\lambda_{\max} \mathbf{u}_{\max}^H \mathbf{u}_{\max} \geq \varepsilon'$ is a necessary condition for the optimization problem. According to [40], the objective function $Tr[(\cdot)^{-1}]$ is convex. Therefore, the above waveform optimization problem (14) is convex. We can obtain the optimal solution directly by using a MATLAB optimization toolbox, such as CVX [40].

However, the proposed scheme is a nonconvex problem in the presence of clutter interference. Then, the objective function in the optimization problem (12) can be rewritten as

$$\begin{aligned}
 f(\mathbf{Z}_i) &= Tr \{ \mathbf{P}_{i|i} \} \\
 &= Tr \left[(\mathbf{P}_{i|i-1})^{-1} + \mathbf{C}_T^{-1} - \left(\mathbf{C}_T + \mathbf{C}_T (\mathbf{Z}_i)^H \mathbf{C}_N^{-1} \mathbf{Z}_i \mathbf{C}_T \right)^{-1} \right]^{-1} \\
 &\simeq Tr \left\{ \left[(\mathbf{P}_{i|i-1})^{-1} + \mathbf{V}_i \mathbf{\Gamma}^H \circ \mathbf{C}_N^{-1} \right]^{-1} \right\}, \tag{17}
 \end{aligned}$$

where $\mathbf{V}_i = (\mathbf{f}_i + \mathbf{a})(\mathbf{f}_i + \mathbf{a})^H$ is real and symmetric and \mathbf{a} is the clutter interference vector. The waveform optimization problem (12) can be rewritten as

$$\begin{aligned}
 \mathbf{V}_i^* &= \arg \min_{\mathbf{V}_i} Tr \left\{ \left[(\mathbf{P}_{i|i-1})^{-1} + \mathbf{V}_i \mathbf{\Gamma}^H \circ \mathbf{C}_N^{-1} \right]^{-1} \right\} \\
 \text{s.t. } Tr \{ \mathbf{V}_i \} &\leq E_f, \quad p(\mathbf{f}_i) = (\mathbf{f}_i + \mathbf{a})^H \mathbf{\Gamma}^H \hat{\mathbf{G}}_i^H \mathbf{C}_N^{-1} \hat{\mathbf{G}}_i \mathbf{\Gamma} (\mathbf{f}_i + \mathbf{a}) \geq \varepsilon'. \tag{18}
 \end{aligned}$$

If $\text{rank}\{\mathbf{V}_i^*\} = 1$, we have $\mathbf{V}_i^* = (\mathbf{f}_0 + \mathbf{a})(\mathbf{f}_0 + \mathbf{a})^H$. The initial waveform \mathbf{f}_0 is the optimal solution. If $\text{rank}\{\mathbf{V}_i^*\} > 1$, since the expression $p(\mathbf{f}_i) \geq \varepsilon'$ is not a convex set, the waveform optimization problem (18) is a nonconvex problem. Then, the expression $p(\mathbf{f}_i) \geq \varepsilon'$ can be rewritten as

$$\mathbf{f}_i^H \mathfrak{N}(\mathbf{r}_{\max}) \geq \sqrt{\varepsilon' / \theta_{\max}}, \tag{19}$$

where θ_{\max} is the maximal eigenvalue of $\mathbf{\Gamma}^H \hat{\mathbf{G}}_i^H \mathbf{C}_N^{-1} \hat{\mathbf{G}}_i \mathbf{\Gamma}$, and \mathbf{r}_{\max} is the corresponding eigenvector. Through eigen-decomposition, we have $\mathbf{\Gamma}^H \hat{\mathbf{G}}_i^H \mathbf{C}_N^{-1} \hat{\mathbf{G}}_i \mathbf{\Gamma} = \sum_k \theta_k \mathbf{r}_k \mathbf{r}_k^H$. As a result, the convex problem is obtained as follows:

$$\begin{aligned} \mathbf{f}_i^* &= \arg \min_{\mathbf{f}_i} \left\| \mathbf{f}_i + \mathbf{a} - \frac{\sqrt{E_f} \mathbf{v}_{\max}}{\|\mathbf{v}_{\max}\|_2} \right\|_2 \\ \text{s.t. } \|\mathbf{f}_i\|_2^2 &\leq E_f, \quad \mathbf{f}_i^H \mathfrak{N}(\mathbf{r}_{\max}) \geq \sqrt{\varepsilon' / \theta_{\max}}, \end{aligned} \tag{20}$$

where \mathbf{v}_{\max} is the eigenvector corresponding to the maximum eigenvalue of \mathbf{V}_i^* . The convex problem can be solved using the optimization toolbox, and \mathbf{f}_i^* is the optimal waveform.

4.2 Closed Targets

The description of TSC is mentioned at the beginning of this section. However, when targets are close to each other, the backscatter signals from different targets are superimposed. The existence of this phenomenon may make it difficult to estimate the TSC. To address this problem, a waveform optimization scheme is proposed by minimizing the MSE of target PSD estimation instead of TSC estimation. The process of waveform optimization for target PSD estimation is shown in Fig. 3.

We employ a wideband radar waveform for illumination in order to implement the target PSD estimation in each frequency sub-band. We consider transmitted waveform $f(t)$ as finite duration, which illuminates multiple extended targets. The j th target signal can be expressed by the convolution of the j th TIR with the transmitted waveform, $s_j(t) = q_j(t) * f(t)$, where $*$ denotes the linear convolution operator. The backscattered signals can be expressed by combining all K target signals with background noise $n(t)$.

$$\begin{aligned} r(t) &= \sqrt{\eta_j} s_j(t) + \sum_{k=1, k \neq j}^K \sqrt{\eta_k} s_k(t) + n(t) \\ &= \sqrt{\eta_j} s_j(t) + g(t) + n(t) \\ &= \sqrt{\eta_j} s_j(t) + c(t), \end{aligned} \tag{21}$$

where η_k is the weight coefficient. We define $Q_j(f_p)$ and $F(f_p)$ as the Fourier transforms of $q_j(t)$ and $f(t)$, respectively, at frequency f_p . $G(f_p)$ is the Fourier transform

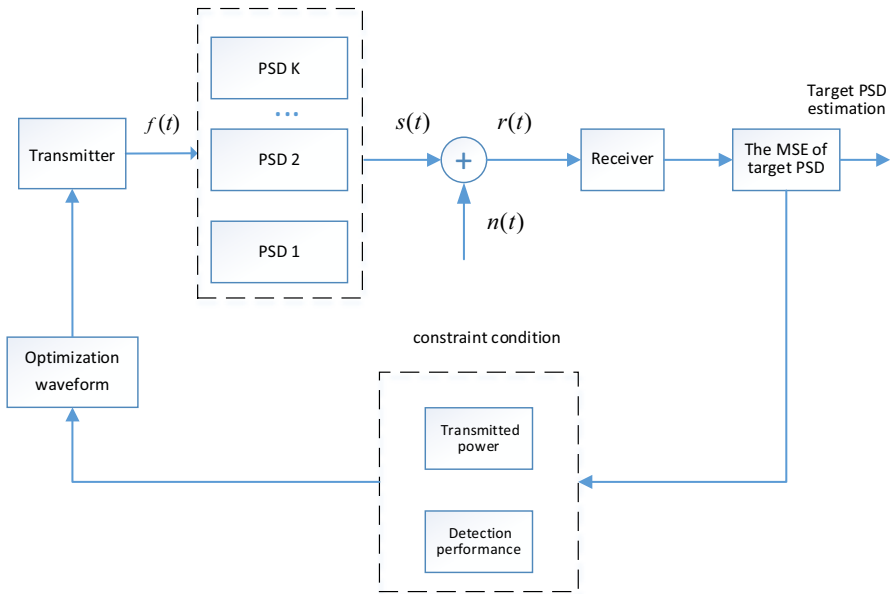


Fig. 3 The process of waveform optimization for target PSD estimation

of $g(t)$ at frequency f_p . The PSD of the j th TIR can be expressed by $P_{q_j}(f) = \left| \int_0^{t_0} q_j(t) e^{j2\pi f t} dt \right|^2$. The PSD of transmitted waveform $F(f_p)$ can be expressed by $P_f(f_p) = F(f_p)F^*(f_p)$, $p = 1, 2, \dots, P$, where p is the number of frequency subbands. During the PSD estimation of the j th target, the echo signals from the other $K - 1$ targets can be modeled as interference. Therefore, the PSD of backscattered signals is presented by the sum of the PSD of the j th target signals and the PSD of the interference and background noise term.

$$\begin{aligned}
 P_r(f_p) &= \eta_j P_{q_j}(f_p) P_f(f_p) + \sum_{k=1, k \neq j}^K \eta_k P_{q_k}(f_p) P_f(f_p) + P_N(f_p) \\
 &= \eta_j P_{q_j}(f_p) P_f(f_p) + P_G(f_p) + P_N(f_p) \\
 &= \eta_j P_{q_j}(f_p) P_f(f_p) + P_C(f_p), \quad p = 1, 2, \dots, P.
 \end{aligned}
 \tag{22}$$

We assume that background noise is WSS Gaussian distributed with known PSD $P_N(f_p) = E\{N(f_p)N^*(f_p)\}$. $N(f_p)$ is the background noise at frequency f_p . $C(f_p) = G(f_p) + N(f_p)$ is the Fourier transform of $c(t)$ at frequency f_p . We considered that $C(f_p)$ follows a complex Gaussian distribution with zero mean and variance, $G_C(f_p) = P_C(f_p)$. Consequently, we have $E\{\hat{P}_C(f_p)\} = G_C(f_p)$. To reduce the computational burden, the target PSD is estimated using a single sample. Then, we define $P_{q_{j,i}}(f_p)$ and $P_{r_{j,i}}(f_p)$ as the PSD of the j th TIR and target signal at time i

and define $Q_{j,i}(f_p)$ and $F_i(f_p)$ as the Fourier transform of $q_j(t)$ and $f(t)$ at time i . Hence, the estimation of $P_{r_{j,i}}(f_p)$ at time i can be expressed as follows:

$$\begin{aligned} \hat{P}_{r_{j,i}}(f_p) &= (\sqrt{\eta_j} Q_{j,i}(f_p) F_i(f_p) + C(f_p)) (\sqrt{\eta_j} Q_{j,i}(f_p) F_i(f_p) + C(f_p))^* \\ &= \eta_j P_{q_{j,i}}(f_p) P_{f_i}(f_p) + \hat{P}_C(f_p) + 2\text{Re}(\sqrt{\eta_j} Q_{j,i}(f_p) F_i(f_p) C(f_p)). \end{aligned} \tag{23}$$

Then, the estimation of $P_{q_{j,i}}(f_p)$ at time i can be written as follows:

$$\hat{P}_{q_{j,i}}(f_p) = \frac{\hat{P}_{r_{j,i}}(f_p) - E\left\{\hat{P}_C(f_p) + 2\text{Re}(\sqrt{\eta_j} Q_{j,i}(f_p) F_i(f_p) C(f_p))\right\}}{P_{f_i}(f_p)}. \tag{24}$$

The radar target echoes are assumed to be independent of each other and the background noise, that is, $E\{\text{Re}(Q_{j,i}(f_p) F_i(f_p) C(f_p))\} = 0$. Then, the above Eq. (24) can be rewritten as follows:

$$\begin{aligned} \hat{P}_{q_{j,i}}(f_p) &= \frac{\hat{P}_{r_{j,i}}(f_p) - G_C(f_p)}{P_{f_i}(f_p)} \\ &= P_{q_{j,i}}(f_p) + \frac{\hat{P}_C(f_p) + 2\text{Re}(\sqrt{\eta_j} Q_{j,i}(f_p) F_i(f_p) C(f_p)) - G_C(f_p)}{P_{f_i}(f_p)}. \end{aligned} \tag{25}$$

Note that the target echoes are also independent of the background noise. The MSE of the j th target PSD estimation at time i can be expressed as follows (see [Appendix B](#)):

$$\begin{aligned} E\left(\|e(f)\|_2^2\right) &= \sum_{p=1}^P E\left(P_{q_{j,i}}(f_p) - \hat{P}_{q_{j,i}}(f_p)\right)^2 \\ &= \sum_{p=1}^P \left[\frac{G_C^2(f_p)}{P_{f_i}^2(f_p)} + \frac{2\eta_j G_C(f_p) P_{q_{j,i}}(f_p)}{P_{f_i}(f_p)} \right]. \end{aligned} \tag{26}$$

From the above Eq. (26), the MSE of the j th target PSD estimation increases with the decrease in $P_{f_i}(f_p)$. If $P_{f_i}(f_p)$ is small, the MSE of the j th target PSD estimation may be large. To ensure the estimation performance, we consider $P_{f_i}(f_p)$ in each frequency sub-band f_p to be no less than a specified threshold E_T . During the i th pulse sample, the waveform design for the j th target estimation is implemented by minimizing the MSE of the j th target PSD estimation. The waveform optimization problem can be described as follows:

$$\min_{P_{f_i}} \sum_{p=1}^P \left[\frac{G_C^2(f_p)}{P_{f_i}^2(f_p)} + \frac{2\eta_j G_C(f_p) P_{q_{j,i}}(f_p)}{P_{f_i}(f_p)} \right]$$

$$\text{s.t. } \Delta f \sum_{p=1}^P P_{f_i}(f_p) = E_f, \quad P_{f_i}(f_p) \geq E_T, \quad P_d \geq \varepsilon, \quad (27)$$

where Δf is the sub-bandwidth and E_f is the transmit power. The expression $P_d \geq \varepsilon$ can be expressed by $Z_i^H \hat{\mathbf{G}}_i^H \mathbf{R}_N^{-1} \hat{\mathbf{G}}_i Z_i \geq \varepsilon'$. Then, the optimization problem (27) can be rewritten as follows:

$$\begin{aligned} & \min_{P_{f_i}} \sum_{p=1}^P \left[\frac{G_C^2(f_p)}{P_{f_i}^2(f_p)} + \frac{2\eta_j G_C(f_p) P_{q_{j,i}}(f_p)}{P_{f_i}(f_p)} \right] \\ & \text{s.t. } \Delta f \sum_{p=1}^P P_{f_i}(f_p) = E_f, \quad P_{f_i}(f_p) \geq E_T, \quad Z_i^H \hat{\mathbf{G}}_i^H \mathbf{R}_N^{-1} \hat{\mathbf{G}}_i Z_i \geq \varepsilon'. \end{aligned} \quad (28)$$

Obviously, the above Eq. (28) is a convex optimization problem. The Lagrange multiplier λ is employed to satisfy the transmit power constraint.

$$H(P_{f_i}(f_p), \lambda) = \frac{G_C^2(f_p)}{P_{f_i}^2(f_p)} + \frac{2\eta_j G_C(f_p) P_{q_{j,i}}(f_p)}{P_{f_i}(f_p)} + \lambda \left(\frac{E_f}{\Delta f} - \sum_{p=1}^P P_{f_i}(f_p) \right). \quad (29)$$

Taking the gradient of (29) with respect to $P_{f_i}(f_p)$ and making it equal to zero, $\frac{\partial H(P_{f_i}(f_p), \lambda)}{\partial P_{f_i}(f_p)} = 0$. From Ref. [38], the optimal solution to (29) can be obtained as follows:

$$\hat{P}_{f_i}(f_p) = \sqrt[3]{-\frac{P_N^2(f_p)}{\lambda} + \sqrt{u}} + \sqrt[3]{-\frac{P_N^2(f_p)}{\lambda} - \sqrt{u}}, \quad (30)$$

where $u = \sqrt{\frac{P_N^4(f_p)}{\lambda^2} + \frac{8P_N^3(f_p) \left(\sum_{k=1}^K \eta_k P_{q_{k,i}}(f_p) \right)^3}{27\lambda^3}}$. The above Eq. (30) is a monotonic function and single-variable optimization problem, which can be implemented via the dichotomy method. The procedure of waveform optimization for target PSD estimation is summarized as Algorithm 2 in Table 2.

In this paper, we assume that all radar targets have a similar reflection characteristic. To simplify the discussion, if the multiple targets always overlap each other during the entire observation period, the reflection characteristics of the radar scene can be regarded as time-invariant. The target PSD, viewed as long-term memory, can be used in transmit waveform design for a relatively long time.

In summary, we aim to explore the waveform optimization for an adaptive radar system under a multitarget scenario. There are two scenarios to consider: multiple extended targets separated in range and multiple extended targets close in range. We propose a waveform optimization scheme based on Kalman filtering by minimizing

Table 2 Waveform Optimization for target PSD estimation (Algorithm 2)

Initializing iteration index $t = 1, \lambda_{\max}, \lambda_{\min}$ and tolerance α

Step 1: $t = t + 1, \lambda_t = \frac{\lambda_{\max} + \lambda_{\min}}{2}$, calculate the PSD of optimized waveform $P_{f_p,t}(f_p, \lambda_t)$.

Step 2: Calculate the power of optimized waveform $E_t = \sum_{p=1}^P P_{f_p,t}(f_p, \lambda_t) \Delta f$.

Step 3: If $|E_t - E_f|/E_f \leq \alpha$, output optimal solution $P_{f,t}(f) = P_{f,t}(f, \lambda_t)$.

Step 4: If $E_t = E_f$ end; otherwise, repeat Step 1

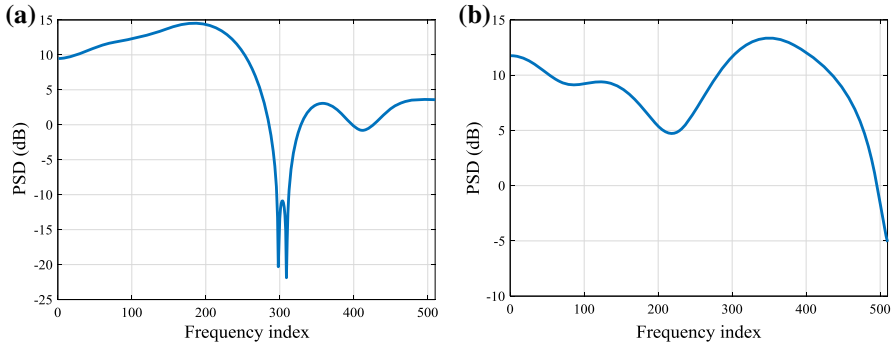


Fig. 4 a The PSD of Target 1; **b** the PSD of Target 2

Table 3 Simulation parameters

E_f	Transmitted power	1
L	Length of signal	30
τ	Temporal correlation	0.1 s
M	Pulse interval	1 ms
p_d	Detection probability	0.95
N	Target number	2

the MSE of separated TSC estimation and a waveform optimization approach by minimizing the MSE of closed target PSD estimation.

5 Simulation

In this section, we simulate Algorithm 1 by minimizing the MSE of TSC estimation and Algorithm 2 by minimizing the MSE of target PSD estimation. We consider two extended targets with different TSC and PSD. We define $\mathbf{g}_k (k = 1, 2)$ as the TSC of the k th target. $\mathbf{g}_k \sim \mathbf{N}(0, \mathbf{C}_{T,k})$ denotes a zero-mean complex Gaussian vector with covariance matrix $\mathbf{C}_{T,k}$. The PSDs of two targets are depicted in Fig. 4a, b.

The center frequency is 10 GHz, and the bandwidth is 500 MHz. The number of sub-bands is 500, and the sub-bandwidth is 1 MHz. The simulation parameters are reported in Table 3.

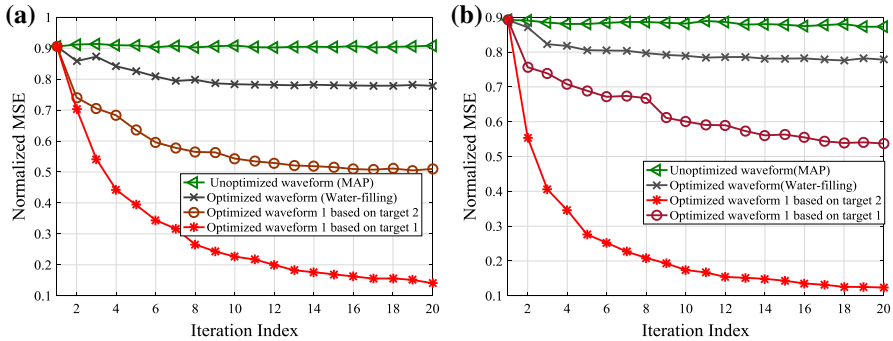


Fig. 5 The normalized MSE of separated TSC estimation **a** Target 1 and **b** Target 2

5.1 Separated Targets

We employ three kinds of transmit waveforms to compare the performance of TSC estimation: (1) the random waveform based on the MAP criterion, (2) the optimized waveform employing the water-filling method, and (3) the optimized waveform employing the proposed Algorithm 1. Eight hundred simulations have been run for each at a particular value of the received SNR. We simulate the proposed Algorithm 1 by using the scattering characteristics of the first and second targets. The performances of TSC estimation for the first and second targets are shown in Fig. 5a, b, respectively.

Figure 5a, b indicates the normalized MSE with regard to TSC estimation under the constraint of detection probability in multipath environments [41, 42]. We discuss the problem of estimating multitarget parameters in diffuse multipath environments, modeling the target echo as the superposition of multiple time-varying signals (due to multiple direct paths) as shown in Eq. (4).

Figure 5a shows that for Target 1, the normalized MSE of TSC estimation provided by the proposed Algorithm 1 is less than the one using the MAP criterion and the water-filling method. Similarly, from Fig. 5b, for Target 2, the performance of TSC estimation generated by the proposed Algorithm 1 is improved by several times compared with the MAP criterion and the water-filling method after 20 iterations.

Because the proposed Algorithm 1 utilizes the temporal correlation of TSC during the pulse interval, the proposed radar system adapts its probing signal to the fluctuating target RCS. On the other hand, the optimized waveform provided by the water-filling method is unable to match the time-varying TSC after multiple iterations. Therefore, the estimation performance provided by the proposed Algorithm 1 is optimal in this case.

To make a trade-off between two targets, we use the vector η to assign weights of separated targets dynamically. The performances of TSC estimation for two targets with different weight coefficients are shown in Fig. 6a, b: (a) the normalized MSE of TSC estimation for Target 1 and (b) the normalized MSE of TSC estimation for Target 2. As shown in Fig. 6a, b, the estimation performance is improved by increasing the weight coefficient of the corresponding target after the first small iteration.

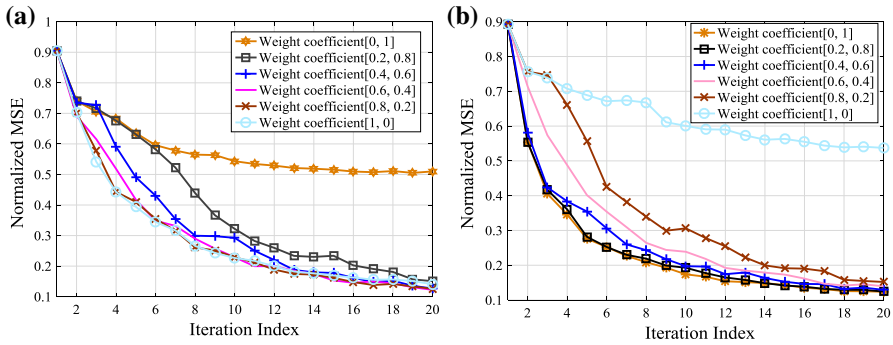
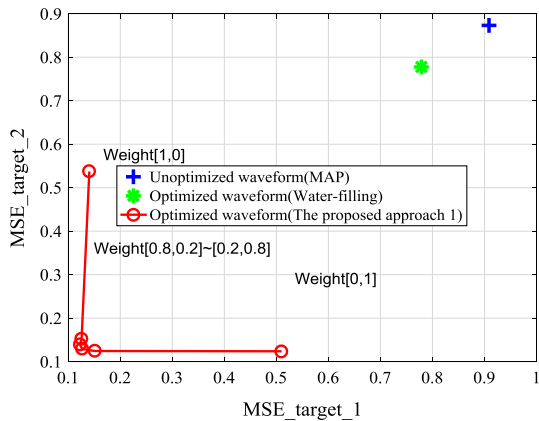


Fig. 6 The normalized MSE of TSC estimation with different weight coefficients a Target 1 and b Target 2

Fig. 7 The joint normalized MSE of separated TSC estimation



For the joint waveform design consideration, vector η is adopted to assign the weights of different targets. The joint normalized MSE of TSC estimation for two separated targets is depicted in Fig. 7. The curve is generated at the end of 20 iterations. The + denotes the random waveform based on the MAP criterion; the * denotes the optimized waveform employing the water-filling method; and o denotes the optimized waveform employing the proposed Algorithm 1. Multiple red points denote the estimation performance of two targets with different vectors of weight coefficients ($\eta = [1, 0]$; $\eta = [0.8, 0.2]$; $\eta = [0.6, 0.4]$; $\eta = [0.4, 0.6]$; $\eta = [0.2, 0.8]$; $\eta = [0, 1]$). As we can observe from Fig. 7, when the weight coefficients are between $[0.8, 0.2]$ and $[0.2, 0.8]$, the curve of the joint normalized MSE provided by the proposed Algorithm 1 is at the lower-left corner. The normalized MSE of TSC estimation generated by the proposed Algorithm 1 is approximately 0.15, compared with 0.78 offered by the water-filling method and 0.86 generated by the MAP criterion. The optimized waveform generated by the proposed Algorithm 1 has the best estimation performance. No significant improvement was observed after 20 iterations.

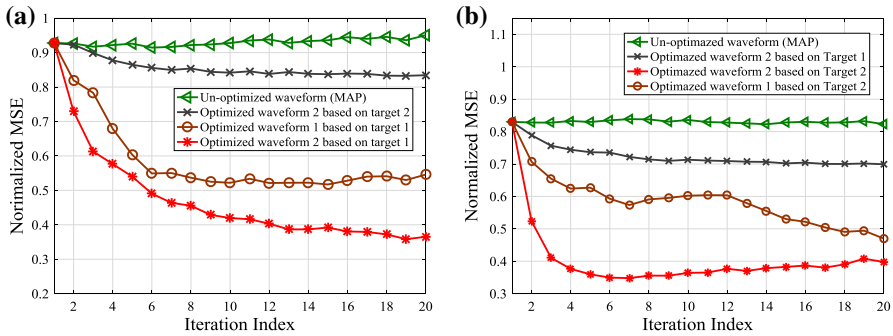


Fig. 8 The normalized MSE of close-target PSD estimation **a** Target 1 and **b** Target 2

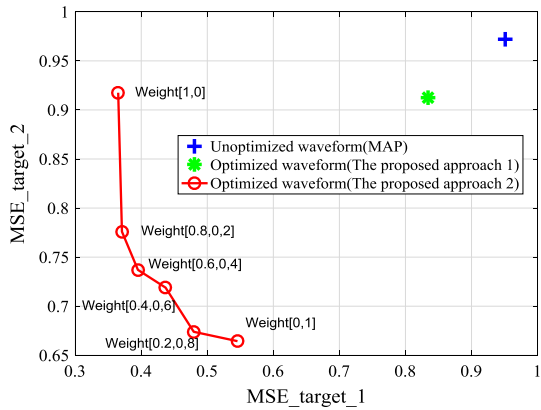
5.2 Closed Targets

We demonstrate the benefits of the proposed Algorithm 2 for target PSD estimation. We employ three types of transmit waveforms to compare the performance of target PSD estimation: (1) the random waveform based on the MAP criterion; (2) the optimized waveform generated by the proposed Algorithm 1; and (3) the optimized waveform generated by the proposed Algorithm 2. Eight hundred simulations have been run for each at a particular value of the received SNR. The performances of target PSD estimation for the first and second targets are shown in Fig. 8a, b, respectively.

Figure 8a, b indicates the normalized MSE of close-target PSD estimation under the constraint of detection probability in multipath environments. The notations are the same as that in Fig. 6. These plots demonstrate an improved MSE performance generated by the proposed Algorithm 2 compared with the MAP method and the proposed Algorithm 1. As can be observed from Fig. 8a, for Target 1, the normalized MSE of target PSD estimation generated by the proposed Algorithm 2 is improved by 25% compared with the proposed Algorithm 1. Similarly, from Fig. 8b, for Target 2, the normalized MSE of TSC estimation generated by the proposed Algorithm 2 is improved by 20% compared with the proposed Algorithm 1. The performance of TSC estimation generated by the proposed Algorithm 2 is improved by 75% compared with the MAP method after 20 iterations. The optimized waveform generated by the proposed Algorithm 2 is able to increase the energy of the target echo, which is useful for target estimation.

The joint normalized MSE of PSD estimation for two closed targets is depicted in Fig. 9. The curve is generated at the end of 20 iterations. The notations are the same as those in Fig. 7. When the weight coefficients are between $[0.6, 0.4]$ and $[0.4, 0.6]$, the curve of the joint normalized MSE generated by the proposed Algorithm 2 is at the lower-left corner. The normalized MSE of PSD estimation generated by the proposed Algorithm 2 is approximately 0.7 compared with 0.91 offered by the proposed Algorithm 1 ($\eta = [0.8, 0.2]$). The normalized MSE of TSC estimation generated by the proposed Algorithm 2 and Algorithm 1 are compared to verify the efficiency of the proposed Algorithm 2 at each iteration step.

Fig. 9 The joint normalized MSE of closed target PSD estimation



6 Conclusions

We have proposed a waveform optimization scheme based on Kalman filtering by minimizing the MSE of separated TSC estimation, in addition to a waveform design scheme based on minimizing the MSE of close-target PSD estimation. An adaptive feedback loop enables the delivery of parameter estimation to the transmitter. The radar system updates the parameter estimation and utilizes this information to choose the optimal waveform for illumination. Finally, subject to the transmitted power and detection probability constraints, the simulation results demonstrate that the proposed schemes provide higher performance gains in terms of TSC estimation and target PSD estimation while still maintaining relatively lower computational complexity.

Acknowledgements This work was supported by the national Natural Science Foundation of China (61761019, 61861017, 61861018, 61862024) and the Natural Science Foundation of Jiangxi Province (Jiangxi Province natural Science Fund) (20181BAB211014, 20181BAB211013), and Foundation of Jiangxi Educational Committee of China (GJJ170414).

Appendix A: Derivation of the Probability Constraints in (12)

Since the true TSC is unknown, the estimate of TSC based on Kalman filtering is used to replace the true TSC to design the radar waveform. We assume that H_1 and H_0 are the presence and absence of a target, respectively. Then, the distribution of backscattered signals can be expressed as

$$\begin{aligned}
 \mathbf{Y}_i|H_0 &\sim \mathbf{N}\{0, \mathbf{C}_N\}, \\
 \mathbf{Y}_i|H_1 &\sim \mathbf{N}\{Z_i \hat{\mathbf{G}}_i, \mathbf{C}_N\},
 \end{aligned}
 \tag{31}$$

where $\hat{\mathbf{G}}_i$ is the estimate of TSC. The likelihood estimation is

$$l(\mathbf{Y}_i) = \frac{\mathbf{N}\{Z_i \hat{\mathbf{G}}_i, \mathbf{C}_N\}}{\mathbf{N}\{0, \mathbf{C}_N\}} \underset{H_2}{\overset{H_1}{\leq}} T$$

$$\Leftrightarrow \mathbf{Y}_i^H \mathbf{C}_N^{-1} Z_i \hat{\mathbf{G}}_i \underset{H_2}{\overset{H_1}{\leq}} T, \quad (32)$$

where T is the detection threshold. The false alarm probability of CFAR detection is

$$P_{fa} = P\left(\mathbf{W}^H \mathbf{C}_N^{-1} Z_i \hat{\mathbf{G}}_i \geq T\right)$$

$$= Q\left(T / \sqrt{(Z_i \hat{\mathbf{G}}_i)^H \mathbf{C}_N^{-1} Z_i \hat{\mathbf{G}}_i}\right). \quad (33)$$

$Q(\cdot)$ is the Q-function. The detection threshold is $T = Q^{-1}(P_{fa}) \sqrt{(Z_i \hat{\mathbf{G}}_i)^H \mathbf{C}_N^{-1} Z_i \hat{\mathbf{G}}_i}$. The probability of detection can be rewritten as

$$P_d = P\left(\left(Z_i \hat{\mathbf{G}}_i + \mathbf{W}\right)^H \mathbf{C}_N^{-1} Z_i \hat{\mathbf{G}}_i \geq T\right)$$

$$= Q\left(Q^{-1}(P_{fa}) - \sqrt{(Z_i \hat{\mathbf{G}}_i)^H \mathbf{C}_N^{-1} Z_i \hat{\mathbf{G}}_i}\right). \quad (34)$$

Since the Q-function describes a monotonically decreasing function, the expression $P_d \geq \varepsilon$ can be rewritten as

$$Z_i^H \hat{\mathbf{G}}_i^H \mathbf{C}_N^{-1} \hat{\mathbf{G}}_i Z_i \geq \varepsilon'. \quad (35)$$

Appendix B: Derivation of (26)

The estimation error of $P_{q_j,i}(f_p)$ can be expressed as

$$e(f_p) = P_{q_j,i}(f_p) - \hat{P}_{q_j,i}(f_p)$$

$$= \frac{G_C(f_p) - \hat{P}_C(f_p) - 2\text{Re}(\sqrt{\eta_j} Q_{j,i}(f_p) F_i(f_p) C(f_p))}{P_{f_i}(f_p)}. \quad (36)$$

The MSE of the j th target PSD estimation at time i can be expressed by

$$E\left(\|e(f)\|_2^2\right) = \sum_{p=1}^P E\left(P_{q_j,i}(f_p) - \hat{P}_{q_j,i}(f_p)\right)^2$$

$$= \sum_{p=1}^P \frac{1}{P_{f_i}^2(f_p)} E\left\{G_C(f_p) - \hat{P}_C(f_p) - 2\text{Re}(\sqrt{\eta_j} Q_{j,i}(f_p) F_i(f_p) C(f_p))\right\}^2$$

$$= \sum_{p=1}^P \frac{1}{P_{f_i}^2(f_p)} E \left(\begin{aligned} & \left(G_C(f_p) - \hat{P}_C(f_p) \right)^2 + 4\eta_j \left(\operatorname{Re}(Q_{j,i}(f_p) F_i(f_p) C(f_p)) \right)^2 \\ & - 4\operatorname{Re}(\sqrt{\eta_j} Q_{j,i}(f_p) F_i(f_p) C(f_p)) \left(G_C(f_p) - \hat{P}_C(f_p) \right) \end{aligned} \right). \quad (37)$$

In (37), we have

$$E \left(\left(G_C(f_p) - \hat{P}_C(f_p) \right)^2 \right) = G_C^2(f_p). \quad (38)$$

$$E \left(\operatorname{Re}(Q_{j,i}(f_p) F_i(f_p) C(f_p)) \left(G_C(f_p) - \hat{P}_C(f_p) \right) \right) = 0. \quad (39)$$

$$E \left(4\eta_j \operatorname{Re}(Q_{j,i}(f_p) F_i(f_p) C(f_p))^2 \right) = 2\eta_j G_C(f_p) P_{q_{j,i}}(f_p) P_{f_i}(f_p). \quad (40)$$

Substituting (38)–(40) into (37), we have

$$E \left(\|e(f)\|_2^2 \right) = \sum_{p=1}^P \left[\frac{G_C^2(f_p)}{P_{f_i}^2(f_p)} + \frac{2\eta_j G_C(f_p) P_{q_{j,i}}(f_p)}{P_{f_i}(f_p)} \right]. \quad (41)$$

References

- Haykin, S.: Cognitive radar: “a way of the future”. *IEEE Signal Process. Mag.* **23**(1), 30–40 (2006)
- Haykin, S.: *Cognitive Dynamic Systems: Perception-Action Cycle, Radar and Radio*. Cambridge University Press, Cambridge (2012)
- Farina, A., De Maio, A., Haykin, S.: *The Impact of Cognition on Radar Technology*. Scitech Publishing, IET (2017)
- Aubry, A., Demaio, A., Farina, A., Wicks, M.: Knowledge-aided (potentially cognitive) transmit signal and receive filter design in signal-dependent clutter. *IEEE Trans. Aerosp. Electron. Syst.* **49**(1), 93–117 (2013)
- Zhang, J.D., Zhu, D.Y., Zhang, G.: Adaptive compressed sensing radar oriented toward cognitive detection in dynamic sparse target scene. *IEEE Trans. Signal Process.* **60**(4), 1718–1729 (2012)
- Patton, L.K., Frost, S.W., Rigling, B.D.: Efficient design of radar waveforms for optimized detection in colored noise. *IET Radar Sonar Navig.* **6**(1), 21–29 (2012)
- Romero, R.A., Goodman, N.A.: Waveform design in signal-dependent interference and application to target recognition with multiple transmissions. *IET Radar Sonar Navig.* **3**(4), 328–340 (2009)
- Gong, X.H., Meng, H.D., Wei, Y.M., Wang, X.Q.: Phase-modulated waveform design for extended target detection in the presence of clutter. *Sensors* **11**(7), 7162–7177 (2011)
- Aubry, A., Carotenuto, V., Maio, A.D.: Optimization theory-based radar waveform design for spectrally dense environments. *IEEE Aerosp. Electron. Syst. Mag.* **31**(12), 14–25 (2017)
- Aubry, A., De Maio, A., Naghsh, M.M.: Optimizing radar waveform and Doppler filter bank via generalized fractional programming. *IEEE J. Sel. Top. Signal Process.* **9**(8), 1387–1399 (2015)
- Karbasi, S.M., Aubry, A., Carotenuto, V., Naghsh, M.M., Bastani, M.H.: Knowledge-based design of space-time transmit code and receive filter for a multiple-input-multiple-output radar in signal-dependent interference. *IET Radar Sonar Navig.* **9**(8), 1124–1135 (2015)
- Aubry, A., De Maio, A., Piezzo, M., Farina, A.: Radar waveform design in a spectrally crowded environment via nonconvex quadratic optimization. *IEEE Trans. Aerosp. Electron. Syst.* **50**(2), 1138–1152 (2014)

13. Chen, C.Y., Vaidyanathan, P.: MIMO radar waveform optimization with prior information of the extended target and clutter. *IEEE Trans. Signal Process.* **57**(9), 3533–3544 (2009)
14. Chen, P., Wu, L.: System optimization for temporal correlated cognitive radar with EBPSK-based MCPC signal. *Math. Probl. Eng.* **2015**(1), 302083 (2015)
15. Kerahroodi, M.A., Aubry, A., De Maio, A., Naghsh, M.M.: A coordinate-descent framework to design low PSL/ISL sequences. *IEEE Trans. Signal Process.* **65**(22), 5942–5956 (2017)
16. Bell, M.R.: Information theory and radar waveform design. *IEEE Trans. Inf. Theory* **39**(12), 1578–1597 (1993)
17. Garren, D.A., Odom, A.C., Osborn, M.K., Goldstein, J.S.: Full-polarization matched-illumination for target detection and identification. *IEEE Trans. Aerosp. Electron. Syst.* **38**(3), 824–837 (2002)
18. Piezzo, M., Aubry, A., Buzzi, S., De Maio, A., Farina, A.: Non-cooperative code design in radar networks: a game-theoretic approach. *EURASIP J. Adv. Signal Process.* **63**(1), 2013 (2013)
19. Deng, X., Qiu, C., Cao, Z., Morelande, M., Moran, B.: Waveform design for enhanced detection of extended target in signal-dependent interference. *IET Radar Sonar Navig.* **6**(1), 30–38 (2012)
20. Goodman, N.A., Venkata, P.R., Neifeld, M.A.: Adaptive waveform design and sequential hypothesis testing for target recognition with active sensors. *IEEE J. Sel. Top. Signal Process.* **1**(1), 105–213 (2007)
21. Calderbank, R., Howard, S., Moran, B.: Waveform diversity in radar signal processing. *IEEE Signal Process. Mag.* **26**(1), 32–41 (2009)
22. Aubry, A., Maio, A.D., Jiang, B., Zhang, S.Z.: Ambiguity function shaping for cognitive radar via complex quartic optimization. *IEEE Trans. Signal Process.* **61**(22), 5603–5619 (2013)
23. Sen, S., Glover, C.W.: Optimal multicarrier phase-coded waveform design for detection of extended targets. In: *Proceedings of the IEEE Radar Conference 2013, Ottawa, Canada*, pp. 1–2 (2013)
24. Haimovich, A.M., Blum, R.S., Cimini, L.J.: MIMO radar with widely separated antennas. *IEEE Signal Process. Mag.* **25**(1), 116–129 (2008)
25. Sen, S., Nehorai, A.: OFDM-MIMO radar with mutual-information waveform design for low-grazing angle tracking. *IEEE Trans. Signal Process.* **58**(6), 3152–3162 (2010)
26. Maio, A.D., Lops, M.: Design principles of MIMO radar detectors. *IEEE Trans. Aerosp. Electron. Syst.* **43**(1), 886–898 (2007)
27. Karbasi, S.M., Aubry, A., Maio, A.D.: Robust transmit code and receive filter design for extended targets in clutter. *IEEE Trans. Signal Process.* **63**(8), 1965–1976 (2015)
28. Pillai, U., Youla, D.C., Oh, H.S., Guerci, J.R.: Optimum transmit–receiver design in the presence of signal-dependent interference and channel noise. *IEEE Trans. Inf. Theory* **46**(2), 577–584 (2000)
29. Yu, Y., Junhui, Z., Lenan, W.: Adaptive waveform design for MIMO radar-communication transceiver. *Sensors* **18**(6), 1957–1968 (2018)
30. Aubry, A., Maio, A.D., Piezzo, M., Farina, A., Wicks, M.: Cognitive design of the receive filter and transmitted phase code in reverberating environment. *IET Radar Sonar Navig.* **6**(9), 822–833 (2012)
31. Sen, S.: PAPR-constrained pareto-optimal waveform design for OFDM-STAP radar. *IEEE Trans. Geosci. Remote Sens.* **52**(6), 3658–3669 (2014)
32. Luo, Z.Q., Ma, W.K., Anthony, M.C.S., Ye, Y.Y., Zhang, S.Z.: Semidefinite relaxation of quadratic optimization problems. *IEEE Signal Process. Mag.* **27**(3), 20–34 (2010)
33. Dai, F.Z., Liu, H.W., Wang, P.H., Xia, S.Z.: Adaptive waveform design for range-spread target tracking. *Electron. Lett.* **46**(11), 793–796 (2010)
34. Yang, Y., Rick, S.B.: MIMO radar waveform design based on mutual information and minimum mean-square error estimation. *IEEE Trans. Aerosp. Electron. Syst.* **43**(1), 330–343 (2007)
35. Chen, P., Wu, L.: Waveform design for multiple extended targets in temporally correlated cognitive radar system. *IET Radar Sonar Navig.* **10**(1), 398–410 (2015)
36. Cover, T.M., Thomas, J.: *Elements of Information Theory*. John Wiley & Sons, New York (2006)
37. Naghibi, T., Behnia, F.: MIMO radar waveform design in the presence of clutter. *IEEE Trans. Aerosp. Electron. Syst.* **47**(2), 770–781 (2011)
38. Jiu, B., Liu, H., Zhang, L., Wang, Y., Luo, T.: Wideband cognitive radar waveform optimization for joint target radar signature estimation and target detection. *IEEE Trans. Aerosp. Electron. Syst.* **51**(2), 1530–1546 (2015)
39. Leshem, A., Napanstek, O., Nehorai, A.: Information theoretic adaptive radar waveform design for multiple extended targets. *IEEE J. Sel. Top. Signal Process.* **1**(1), 42–55 (2007)
40. Boyd, S.P., Vandenberghe, L.: *Convex Optimization*. Cambridge University Press, Cambridge (2004)

41. Aubry, A., Maio, A.D., Foglia, G.: Diffuse multipath exploitation for adaptive radar detection. *IEEE Trans. Signal Process.* **63**(5), 1268–1281 (2015)
42. Aditya, S., Molisch, A.F., Behairy, H.M.: A survey on the impact of multipath on wideband time-of-arrival-based localization. *Proc. IEEE* **106**(7), 1183–1203 (2018)

Publisher's Note Springer Nature remains neutral with regard to jurisdictional claims in published maps and institutional affiliations